PPPL-CFP--2886
Conf-9305231--2

Observations of Fast Ion Losses Due to Toroidal Alfvén Eigenmodes in TFTR

D. S. Darrow, S. J. Zweben, Z. Chang, C. Z. Cheng, E. D. Fredrickson, E. Mazzucato, R. Nazikian, C. K. Phillips, R. B. White, J. R. Wilson, and K.-L. Wong

Princeton University, Plasma Physics Laboratory
Princeton, NJ 08543
USA

RECEIVED
AUG 25 1993
OSTI

Introduction

In a tokamak, knowledge of the rate of fast ion loss is of importance in determining the energy balance of the discharge. Heating of the discharge may be diminished if losses are significant, since neutral beam ions, ICRF heating tail ions, and alpha particles all heat the plasma and may all be lost through processes which expel fast ions. In addition, a loss of fast ions which is sufficiently intense and localized may damage plasma facing components in the vacuum vessel. For these reasons, knowledge of the fast ion loss mechanisms is desirable.

Loss processes for fast ions in a tokamak fit into two broad categories: single particle and collective. Single particle losses are those, such as first orbit loss, which are independent of the number of fast ions present. These have been seen in numerous instances on TFTR with DD fusion products, and are reported elsewhere [1-4]. Collective losses arise when the fast ion density is sufficient to drive instabilities which then cause loss. The drive can come from $\frac{\partial f_{fi}}{\partial \psi}$ (where f_{fi} is the fast ion distribution function), $\frac{\partial f_{fi}}{\partial E}$, and resonances. Examples of collective instabilities include the toroidal Alfvén eigenmode (TAE), the kinetic ballooning mode (KBM), alpha driven sawteeth, alpha driven fishbones, Alfvén waves, and ion cyclotron waves. This paper limits itself to the presentation of observations made during what are believed to be TAEs which were excited under two conditions in TFTR: at low field (1.5 T), with neutral beam ions driving the mode [5, 6], and at intermediate field (3.4 T), with the hydrogen minority ICRF tail ions driving the mode [7].

The detectors used to measure the fast ion loss were the escaping alpha detectors, which are described elsewhere [1-4, 8]. These detectors act as magnetic spectrometers, dispersing fast ions onto a scintillator, depending upon their gyroradius and pitch angle. The detectors are located at 20°, 45°, 60°, and 90° below the outboard midplane. For the NBI driven TAE, only the 20° probe could be utilized, since the 100 keV deuterons are screened from the other probes by a 3 μm thick aluminum foil which stops particles with energies below ~400 keV; the 20° has no such foil. For the ICRF tail ion driven TAE, the 20°, 45°, and 60° probes all showed measurable signal.

The TAE is a global mode in a tokamak. A single mode is characterized by a single toroidal mode number, n, and several poloidal mode numbers, m, which vary with minor radius. Its frequency is given approximately by $\omega=\frac{v_A}{2qR}$, where v_A is the Alfvén velocity. The mode is driven by the spatial gradient of the fast ion density, and in order for the mode to

MASTER

DISTRIBUTION OF THIS DOCUMENT IS UNLIMITED

be unstable, the fast ion velocity must exceed v_A (although there is some sideband drive of the mode if $v_{fi}>v_A/3$). In addition, the total drive must exceed the total damping.

Neutral Beam Ion Driven TAE

The NBI driven TAE in TFTR appears only when the toroidal field is lowered sufficiently so that the 100 keV beam deuterons satisfy $v_D>v_A$. Under these conditions, an instability is observed on the Mirnov coils which has a frequency of approximately 100 kHz. The mode amplitude increases with increasing NBI power, and the mode vanishes entirely when B_T is raised [5, 6]. Likewise, the frequency scales with density and toroidal field according to the formula for the frequency stated above. Typical parameters for these plasmas are: 1 T $\leq B_T \leq$ 2 T, 300 kA $\leq I_p \leq$ 700 kA, $n_e=3\times10^{19}$ m^{-3}, R=2.40 m, a=0.75 m, β_{fast}~0.5%, and $\langle\beta\rangle$~1%.

Figure 1 shows the time histories of a Mirnov coil signal, the neutron rate, and the rate of neutral beam ion loss to the 20° escaping alpha detector [9]. The bursts in the Mirnov signal are caused by the TAE. During each burst, the beam ion loss rate increases, the amount of the increase being correlated with the size of the Mirnov burst. Likewise, the neutron rate is seen to drop after the larger bursts, indicating an expulsion of beam ions. The time delay between the peak of the Mirnov signal and the peak of the beam ion loss is about 0.5 msec. This interval corresponds to several tens of bounce times, and indicates that the loss mechanism requires numerous transits of the particle through the mode in order to cause expulsion.

Figure 2 compares the losses in the presence and absence of the TAE. In this and all the figures in this paper, the pitch angles quoted are with respect to the toroidal field. Hence, the pitch angle, χ, is defined as $\chi=\arccos(v_{||}/v)$. The pitch angle of the passing/trapped boundary is 47° at the 20° probe for these plasma conditions and particle energies. The case without TAE was taken a short time after the neutral beams had turned off, sufficiently long afterwards that the TAE activity had ceased, but still soon enough that the plasma parameters had not changed substantially. The case with the TAE present is actually averaged over an interval of time which includes several bursts of the mode. With no TAE present, Fig. 2(a), the loss is centered at a pitch angle of 57° and a gyroradius of 7 cm. This gyroradius corresponds, as shown in the figure, to full energy NB ions. Fig. 2(b) shows the loss averaged over several bursts of the TAE. In this case, the peak of the loss has moved to a higher pitch angle, 60°, and a lower gyroradius, 6 cm. The contours are at the same interval as in Fig. 2(a). Fig. 2(c) shows the intensity versus pitch angle for the two cases, again indicating the shift to higher pitch angles when the TAE is present. This shift is consistent with the possible outward major radial transport of the beam ions due to mode-particle resonances, as discussed in the section below on ICRF tail driven TAEs.

Some aspects of this loss are not well understood. For instance, there is a loss of neutral beam ions even when the TAE is absent. This loss is of trapped particles, yet the beam ions are injected on passing orbits. In addition, it is not known whether there are losses of nearly parallel passing beam ions which are undetectable with the probe used—for instance passing particles with pitch angle below 40° are entirely excluded.

H-minority ICRF Tail Driven TAE

Another condition in TFTR in which TAEs can apparently be driven is during H-minority ICRF heating [8]. In such plasmas, the tail ions can exceed the Alfvén velocity and can drive TAEs. Typical plasma parameters are: $B_T = 3.4$ T, 1.3 MA $\leq I_p \leq$ 1.8 MA, R = 2.62 m, a = 1.00 m. He or D plasmas, $\langle n_e \rangle = 2.5\times10^{19}$ m^{-3}, 3 MW $\leq P_{ICRF} \leq$ 11 MW, T_{tail} = 500-600 keV ($v_{tail} \sim v_A \sim 1\times10^7$ m/sec), $\langle \beta \rangle = 0.3\%$, and $\langle \beta_{fast} \rangle = 0.03\%$. The TAEs under these conditions are more in a regime of relevance to reactors (and to TFTR DT) than the NBI driven ones since the toroidal field is higher.

Under these conditions, the TAE appears as a magnetic fluctuation at a frequency between 170 and 250 kHz. The mode is also seen with the microwave reflectometer and it appears only when the ICRF power exceeds 3 MW (equivalently, when the fast ion tail exceeds 70 kJ). The mode frequency scales inversely with the square root of plasma density, in agreement with the equation for the mode frequency. Its scaling with magnetic field cannot be checked convincingly since changing B_T also alters the ICRF resonance location.

Figure 3 displays the time history of a TAE driven by the H-minority tail ions. The top trace depicts the total fast ion loss to the 45° escaping alpha probe versus time. The second trace is the mode amplitude. When the mode appears, the fast ion loss is seen to increase suddenly and substantially. As time progresses, the mode amplitude diminishes, as do the fast ion losses. This, presumably, is due to some evolution of the tail ion distribution. At the sawtooth crashes (seen in the third trace) the mode momentarily turns on, and the losses increase correspondingly. This, it is postulated, is due to a rearrangement of the fast ion profile. This figure also shows the turn-on threshold of 3 MW.

The tail ions which are lost are trapped ions whose energies lie in the range 0.5 to 1 MeV, based upon the gyroradii detected. The lower end of this range, 0.5 MeV, corresponds to protons whose velocities are approximately equal to the Alfvén velocity, as noted above.

Figure 4(a) depicts the mode amplitude, as determined from the Mirnov coils, and the escaping tail ion loss power as functions of the applied ICRF power. Both quantities are strongly increasing functions of the ICRF power. The escaping tail ion loss power is estimated by comparing the magnitude of the loss at the 45° detector to losses of fusion products during an ordinary neutral beam heated shot. By choosing an NBI shot which is MHD quiescent, it may be assumed that the losses of fusion products are due solely to first orbit loss and stochastic toroidal field ripple loss [1-4] and, assuming that the poloidal distributions of the losses in the two types of discharges are the same (admittedly a weak assumption), one can obtain an approximate absolute calibration of the detectors. The percentage of input power lost is then based upon this calibration. The uncertainties in the power loss quoted in Fig. 4(a) are considerable. However, it is possible to conclude, independent of the exact calibration, that a significant amount of power is lost in ICRF tail ions when the TAE amplitude is large. In the worst case shown, with 11 MW of applied ICRF power, an estimated 1 MW is lost due to escaping tail ions.

This substantial loss may help explain two other experimental observations. First, it is seen that the energy stored in fast ions does not increase with ICRF power for powers above 5 MW in helium majority plasmas. It may be that part or all of this additional input power is rapidly lost to the walls in tail ions (the accuracy of the measurements described above does not preclude the possibility that all the additional input power above 5 MW is lost in escaping tail ions). Secondly, some in-vessel components in TFTR which lie between 10 and 30 cm in the shadow of the limiters have been melted or damaged due to excessive heating. This damage is concentrated both near the midplane and in the bottom of the

vessel, between the toroidal field coils. The midplane damage corresponds to where most of the tail ions should be lost due to the TAE, as described below.

Figure 4(b) depicts the same data as in 4(a), but plotted as power loss versus mode amplitude. The relationship between the two quantities is best fit by a straight line. The linear relationship between the two quantities suggests that the loss is due to a process which is convective in nature, rather than diffusive. Observations from the DIII-D tokamak also indicate a linear relationship between TAE amplitude and particle loss rate [10-12]. Computational work [13] predicts loss of a convective character at first, followed by loss of a diffusive nature (loss rate quadratic in mode amplitude) as the most easily lost particles are depleted. This computation may not apply well to this experiment since the parameters used differ significantly from those in the experiment. In particular, the present experiments do not contain an isotropic distribution of fast ions, but one which is dominated by trapped ions. In addition, in the experiment, there is a continual source of new fast ions accelerated by the ICRF waves, while in the simulation there is a population which is depleted and not replenished with time.

Based upon the data from the 90°, 60°, and 45° detectors, the loss of tail ions increases toward the midplane. Unfortunately, the 20° detector is of a different geometry than the others, which makes it quite difficult to compare the fluxes in each probe directly.

Figure 5 shows the orbits of particles which enter the 20°, 45°, and 60° detectors with and without the TAE (the 90° detector sees a negligible signal). The ICRF resonance layer is shown as a vertical line in each figure. In the cases of the 45° and 60° detectors, it can be seen that the TAE causes the pitch angle of the observed loss to increase—i.e. more deeply trapped particles are lost. This was also observed to be the case with the NBI driven TAEs. For the 20° detector, the loss in the absence of the TAE was too small to detect, hence no orbit is plotted for that case. However, during the TAE, a significant loss is seen, with a typical orbit as depicted in Fig. 5(c). The intriguing feature of this data is that particles which must have originated at the ICRF resonance layer now occupy orbits which are far removed from that region.

A loss mechanism which is consistent with these orbit observations is one in which the TAE causes transport of resonant fast ions outward in major radius. Since the bounce frequency of the particles is roughly equal to the TAE frequency, this is possible. The 20° detector data seems especially to support this interpretation, since the tail ions appear radially outward from where they are created, and are moved a substantial distance to the detector within a fraction of a slowing down time. Such a mechanism might also explain the observed linear relationship between loss rate and mode amplitude. A similar mechanism was previously found to be responsible for the expulsion of neutral beam ions during fishbone oscillations [14].

Summary

In summary, TAEs have been observed in TFTR driven both by NBI ions and by H-minority ICRF tail ions. In both cases, the mode characteristics scale as predicted by theory, and in both cases enhanced losses of fast ions are seen coincident with the instability. In the case of the NBI driven TAE, the mode increases the level of losses by up to a factor two, and causes more deeply trapped and slightly less energetic particles to be ejected. In the ICRF tail ion driven TAE, the loss of applied plasma heating power due to the mode can be quite large: up to ~10% of the input power. In the ICRF driven mode, the power lost varied linearly with the mode amplitude. In both types of TAEs, more deeply trapped particles are lost during the mode. This shift in pitch angles is consistent with the

outward major radial transport of mode-resonant ions. Because of the level of losses seen in TFTR and other devices, work is continuing to be done to measure and understand fast ion losses resulting from TAEs. The issue of alpha particle driven TAEs and resulting alpha losses will be studied in TFTR's forthcoming DT experiments.

Acknowledgements

This work was supported by US DoE contract DE-AC02-76-CHO-3073.

References

[1] S. J. Zweben, *Nucl. Fusion* **29**, 825 (1989).

[2] S. J. Zweben, et al., *Nucl. Fusion* **30**, 1551 (1990).

[3] S. J. Zweben, et al. Phys. Fluids B **2**, 1411 (1990).

[4] R. L. Boivin, "Measurements of Charged Fusion Product Diffusion in TFTR," Ph.D. Thesis, Princeton University, October 1991.

[5] K.-L. Wong, et al. *Phys. Rev. Lett.* **66**, 1874 (1991).

[6] K.-L. Wong, et al. *Phys. Fluids B* **4**, 2122 (1992).

[7] R. L. Boivin, S. Kilpatrick, D. Manos, and S. J. Zweben, *Rev. Sci. Instrum.* **61**, 3208 (1990).

[8] J. R. Wilson, et al. in *Proc. of the 14th International Conference on Plasma Physics and Controlled Nuclear Fusion Research*, Wurzburg, Germany, October 1992, paper IAEA-CN-56/E-2-2

[9] D. S. Darrow, et al. *Proc. 19th EPS Conf. on Controlled Fusion and Plasma Physics*, Part I, 431-434 (1992)

[10] W. W. Heidbrink, et al., *Nucl. Fusion* **31**, 1635 (1991).

[11] E. J. Strait, et al., *Nucl. Fusion* **33**, 61 (1993).

[12] H. Duong, et al., General Atomics Report Number GA-A21038 (1993).

[13] D. J. Sigmar et al., *Phys. Fluids B* **4**, 1506 (1992).

[14] R. B. White, et al., *Phys. Fluids* **26**, 2958 (1983).

DISCLAIMER

This report was prepared as an account of work sponsored by an agency of the United States Government. Neither the United States Government nor any agency thereof, nor any of their employees, makes any warranty, express or implied, or assumes any legal liability or responsibility for the accuracy, completeness, or usefulness of any information, apparatus, product, or process disclosed, or represents that its use would not infringe privately owned rights. Reference herein to any specific commercial product, process, or service by trade name, trademark, manufacturer, or otherwise does not necessarily constitute or imply its endorsement, recommendation, or favoring by the United States Government or any agency thereof. The views and opinions of authors expressed herein do not necessarily state or reflect those of the United States Government or any agency thereof.

Figure Captions

Figure 1: Time history of the Mirnov coil signal, the neutron rate, and the rate of beam ion loss for a plasma in which the TAE was driven unstable by 100 keV deuterons from the neutral beam heating system of TFTR.

Figure 2: (a) Detected distribution in pitch angle and gyroradius of beam ion losses just after beam injection and TAE activity ceased in a TAE-unstable discharge. The grid indicates the pitch angle and gyroradii coordinates in the detector. The boundary between passing and trapped particles is at a pitch angle of 47°. (b) Detected distribution from the same discharge, averaged over several TAE bursts. Contour interval is the same as in part (a). (c) The distributions in parts (a) and (b), integrated over gyroradius and plotted versus pitch angle.

Figure 3: Time history of a discharge with H-minority ICRF tail ion driven TAE. (a) Tail ion loss rate at the 45° escaping alpha detector. (b) TAE amplitude from Mirnov coil. (c) Soft X-ray signal showing the sawtooth behavior of the discharge. (d) Applied ICRF power.

Figure 4: (a) TAE amplitude and escaping tail ion loss power versus applied ICRF power. (b) Escaping tail ion loss power versus mode amplitude.

Figure 5: (a) Escaping ICRF tail ion orbits with and without the TAE, as seen at the 60° detector. (b) Escaping ICRF tail ion orbits with and without the TAE, as seen at the 45° detector. (c) Escaping ICRF tail ion orbits during the TAE only, as seen at the 20° detector.

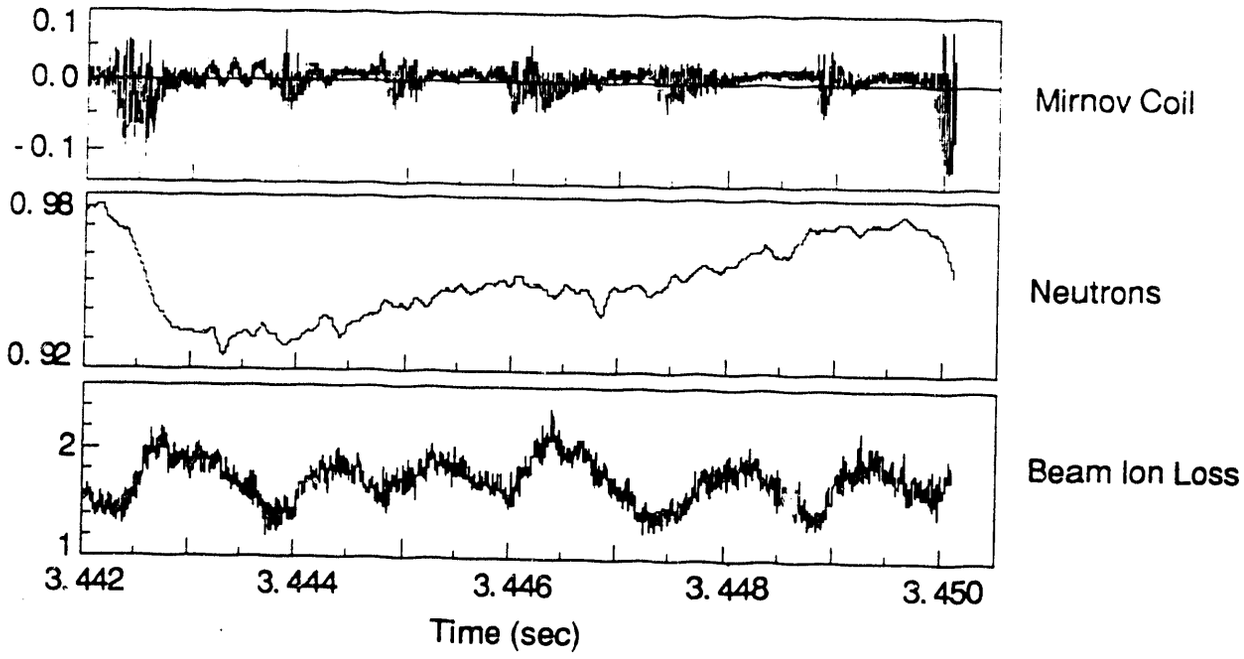
0.1
0.0
-0.1
Mirnov Coil
0.98
0.92
Neutrons
2
1
Beam Ion Loss
3.442
3.444
3.446
3.448
3.450
Time (sec)

Figure 1

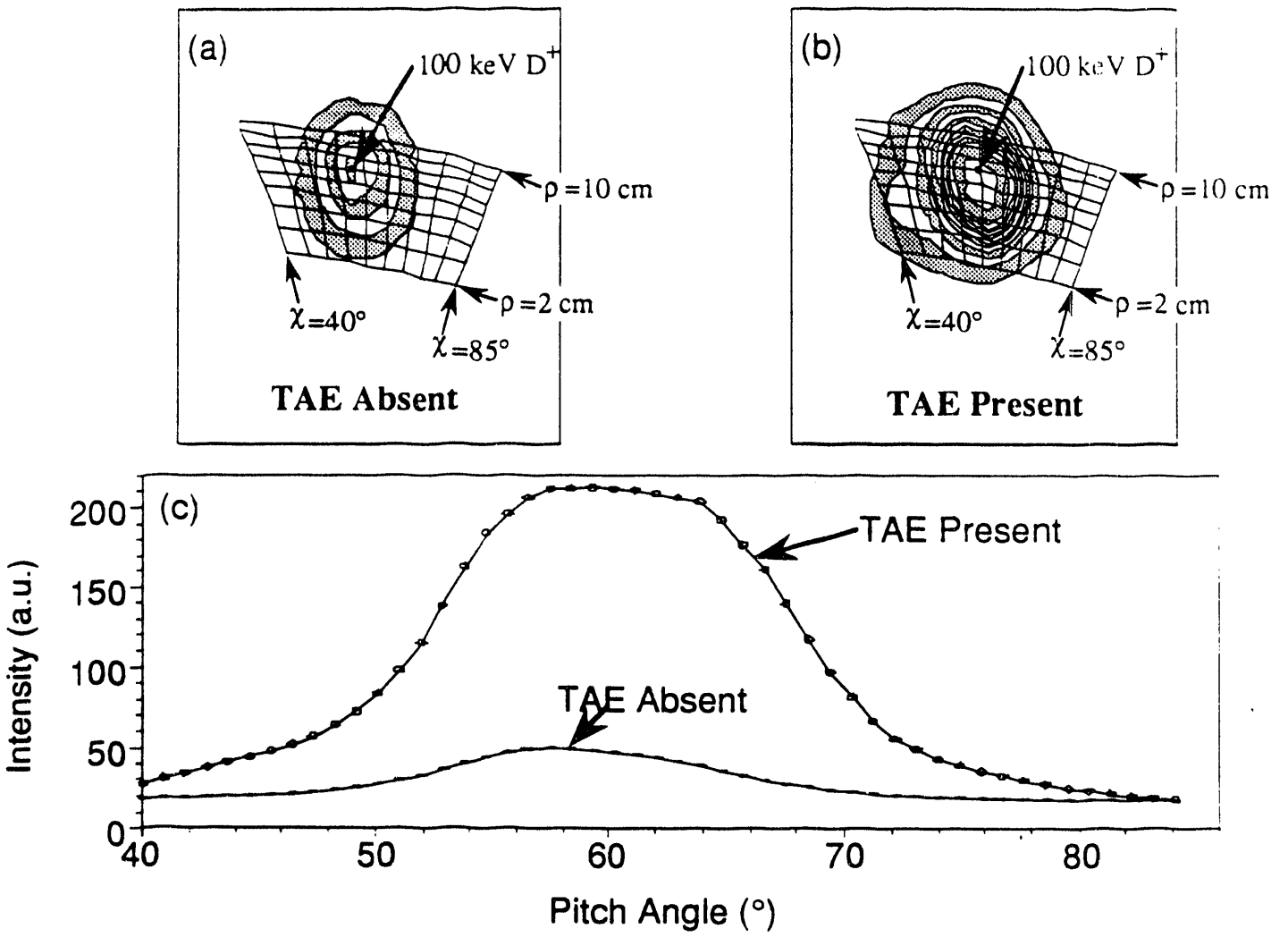
(a)
100 keV D+
ρ=10 cm
ρ=2 cm
χ=40°
χ=85°
TAE Absent
(b)
100 keV D+
ρ=10 cm
ρ=2 cm
χ=40°
χ=85°
TAE Present
(c)
TAE Present
TAE Absent
Intensity (a.u.)
0
50
100
150
200
40
50
60
70
80
Pitch Angle (°)

Figure 2

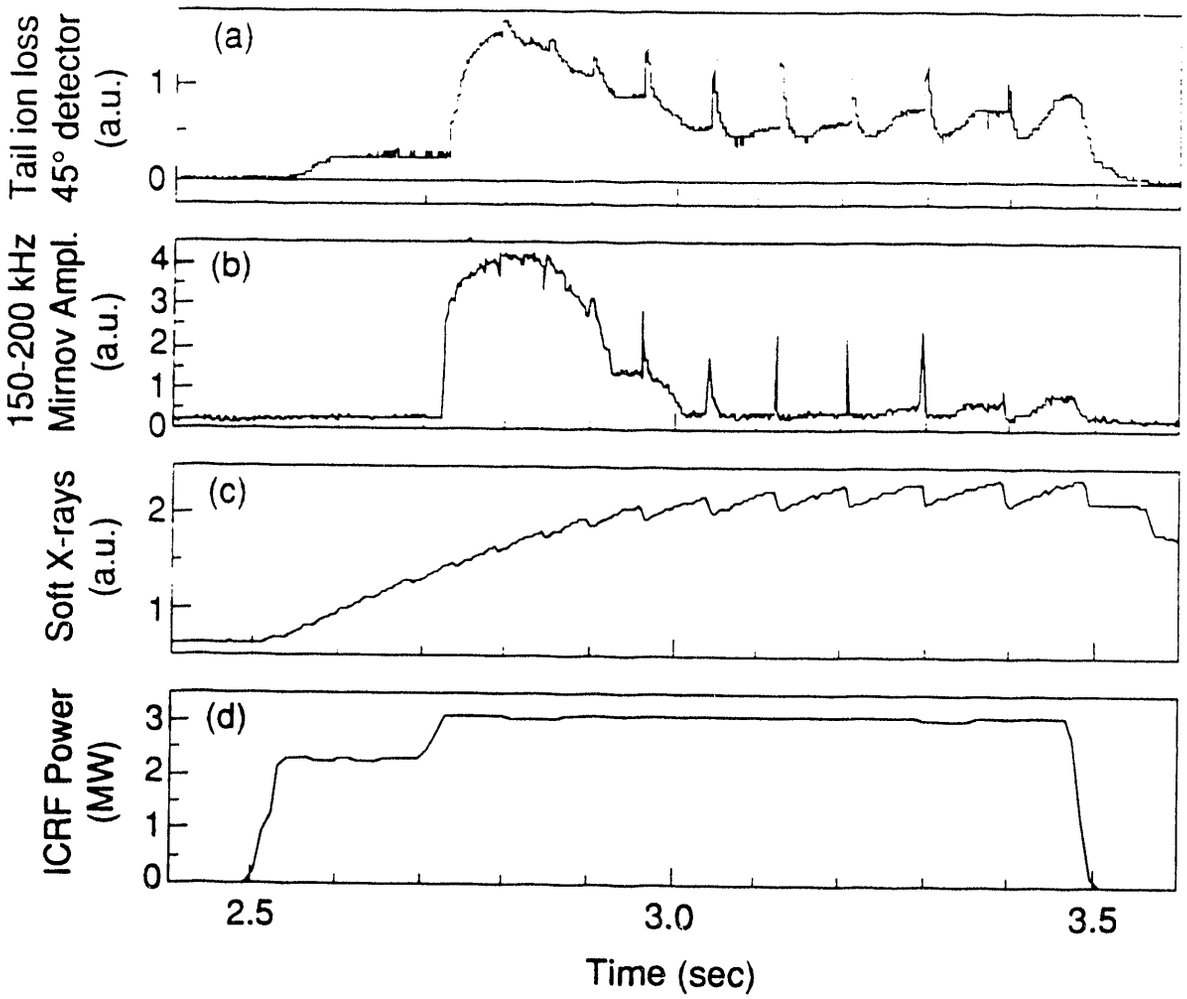
Tail ion loss
45° detector
(a.u.)
(a)
1
0
150-200 kHz
Mirnov Ampl.
(a.u.)
(b)
4
3
2
1
0
Soft X-rays
(a.u.)
(c)
2
1
ICRF Power
(MW)
(d)
3
2
1
0
2.5
3.0
3.5
Time (sec)

Figure 3

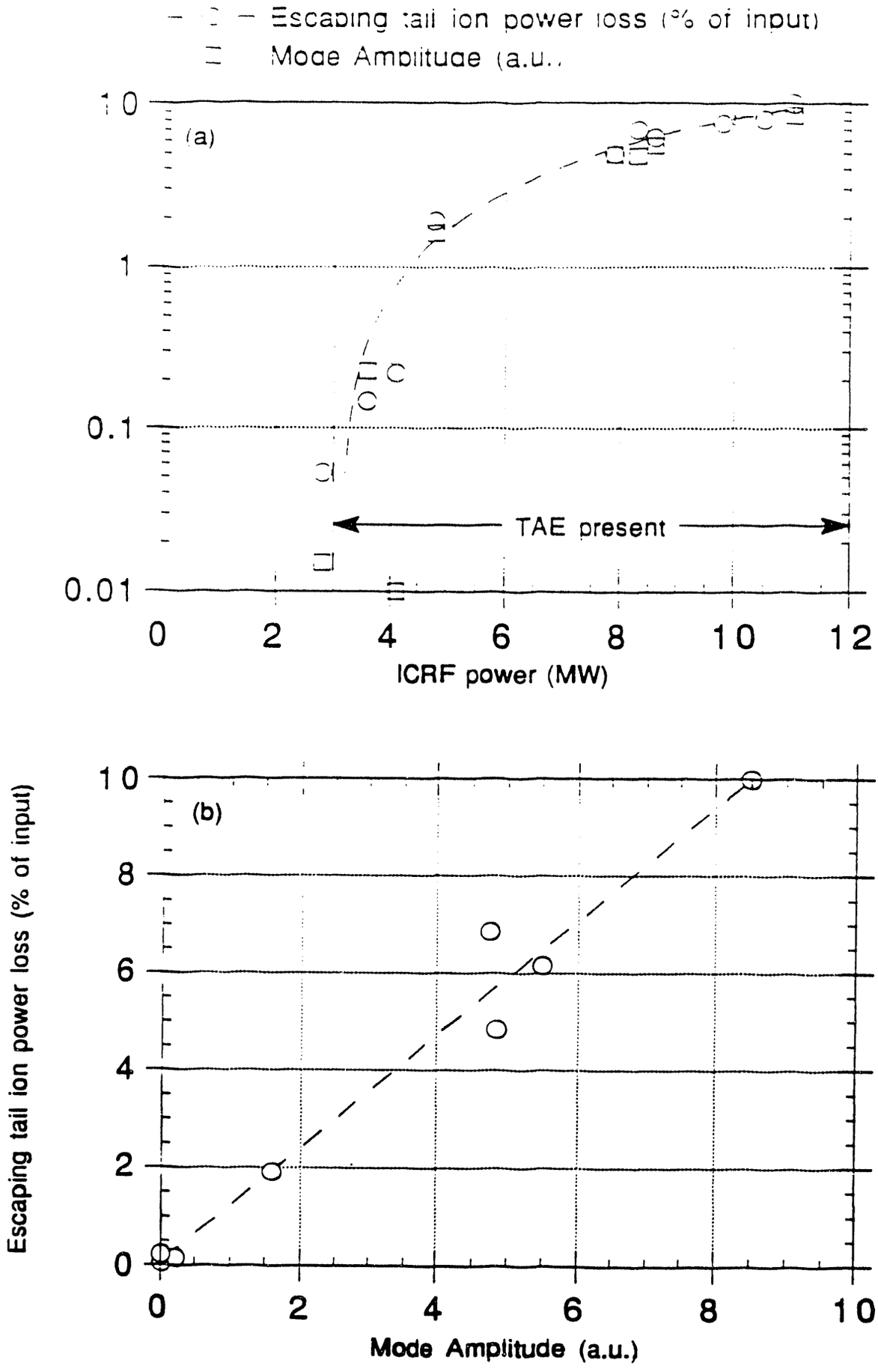
Escaping tail ion power loss (% of input)
Mode Amplitude (a.u.)
(a)
10
1
0.1
0.01
TAE present
0
2
4
6
8
10
12
ICRF power (MW)
(b)
10
8
6
4
2
0
Escaping tail ion power loss (% of input)
0
2
4
6
8
10
Mode Amplitude (a.u.)

Figure 4

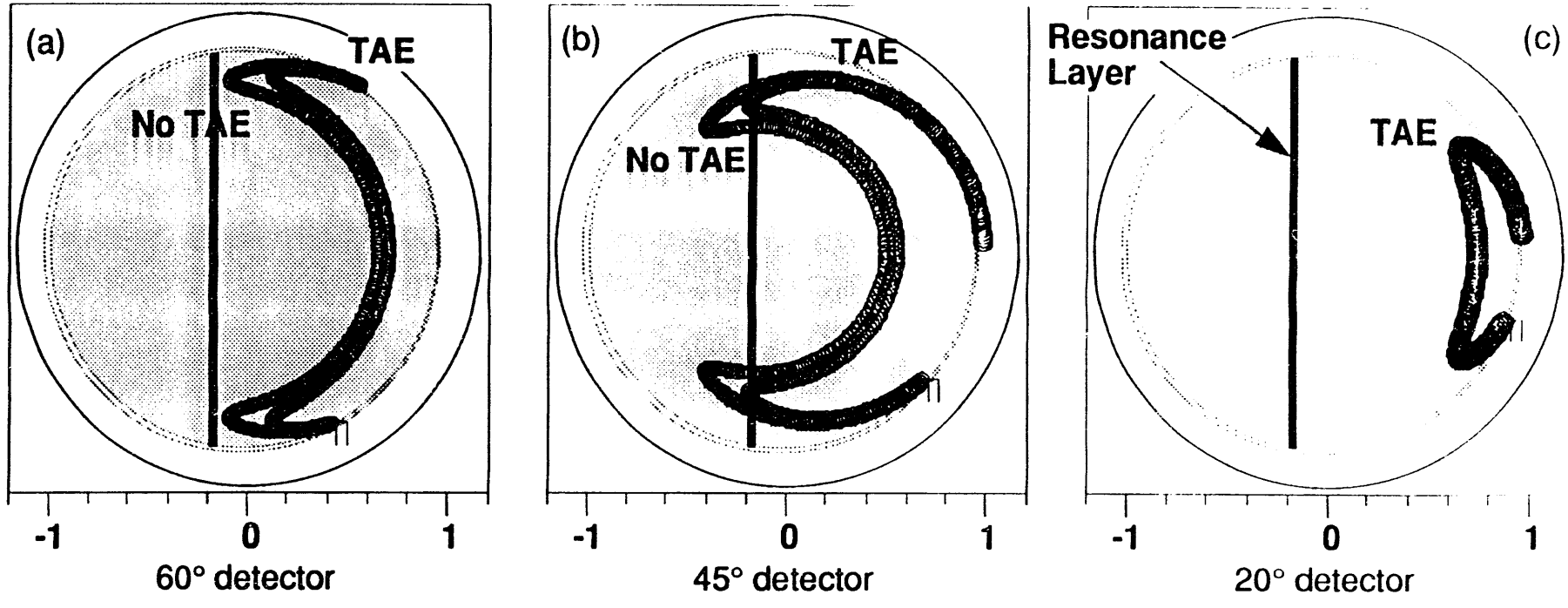
(a)
TAE
No TAE
-1
0
1
60° detector
(b)
TAE
No TAE
-1
0
1
45° detector
Resonance
Layer
(c)
TAE
-1
0
1
20° detector

Figure 5

END

DATE FILMED

11/5/93